Analysis of a California Catalina Eddy Event

LANCE F. BOSART

Department of Atmospheric Science, State University of New York at Albany, Albany, NY 12222

(Manuscript received 15 November 1982, in final form 30 March 1983)

ABSTRACT

During the period 26–29 May 1968 a shallow cyclonic circulation, known locally as a Catalina eddy, developed in the offshore waters of southern California. A synoptic and mesoscale analysis of the event establishes the following: 1) the incipient circulation forms on the coast near Santa Barbara downwind of the coastal mountains, 2) cyclonic shear vorticity appears offshore in response to lee troughing downstream of the coastal mountains between Vandenberg and Pt. Mugu, California, 3) mountain wave activity may be aiding incipient eddy formation in association with synoptic-scale subsidence and the generation of a stable layer near the crest of the coastal mountains, 4) a southeastward displacement and offshore expansion of the circulation occurs following the passage of the synoptic-scale ridge line, and 5) dissipation of the eddy occurs with the onset of a broad onshore flow.

1. Introduction

California meteorologists broadly refer to a Catalina eddy as a mesoscale cyclonic circulation that occurs within the marine layer offshore from southern California. The purpose of this paper is to analyze a case of local interest with emphasis on the mesoscale structure. Prominent topographical and geographical features relevant to this study, in southern California are displayed in Fig. 1.

While a Catalina eddy is a non-event on the meteorological Richter scale, it does have a significant local impact. Largely a spring and summer phenomenon, the eddy circulation alters the typical coastal stratus regime from Baja California northward to beyond Santa Barbara. The evolution of the circulation is accompanied by the development of southerly and southeasterly winds along the aforementioned coastal strip in conjunction with a deepening of the marine layer. The persistent stratus deck thickens and extends inland, sometimes spilling through passes in the coastal mountains. Coastal visibilities improve as the mixed layer deepens and much of the heavy pollution of the Los Angeles basin is advected offshore or through the mountain passes into the desert and vertically mixed through a characteristically deeper marine layer.

The interested reader is referred to Rosenthal (1972) for an extensive discussion of southern California weather regimes in general and the Catalina eddy circulation in particular. The eddy circulation has been attributed to both orographic effects of the coastal mountains between Vandenberg and Santa Barbara and synoptic scale forcing in previous work cited by Rosenthal. The aforementioned earlier investigations have tended to concentrate on climatological aspects of the eddy circulation. In the present study a detailed meteorological analysis is made of the case of 27–29 May 1968. Rosenthal's (1968) satellite note is the motivation for the present work. Figure 2, redrawn from Rosenthal (1968), depicts the evolution of the offshore cloud pattern as seen from the old TIROS satellite pictures. At 1728 GMT 27 May coastal stratus is conspicuously absent from the California coastal waters. By 1523 GMT 28 May this offshore region is mostly covered with shallow stratus clouds. Note the clear areas around the offshore islands. Cloud development continues in the next three hours (1821 GMT) with complete coverage evident by 1716 GMT 29 May. Only the highest areas of some of the channel islands (visible in the original pictures) are still visible, indicative of a deepening of the marine layer and probable thickening of the stratus deck. The May 1968 case is attractive for further research because the availability of conventional radiosonde data is much superior to that of today. Soundings were regularly available from Vandenberg (72393) and San Nicholas Island (72391) four and two times daily, respectively. Additional soundings were available from Pt. Mugu (72391) and China Lake (74612) at frequent, but sometimes irregular intervals.

2. Synoptic overview

A series of subjectively drawn 700 and 200 mb maps at 48 h intervals encompassing the period 0000 GMT 25–29 May 1968 is shown in Fig. 3. Initially a diffluent flow pattern is seen along the west coast of the United States at 700 mb accompanying a mi-

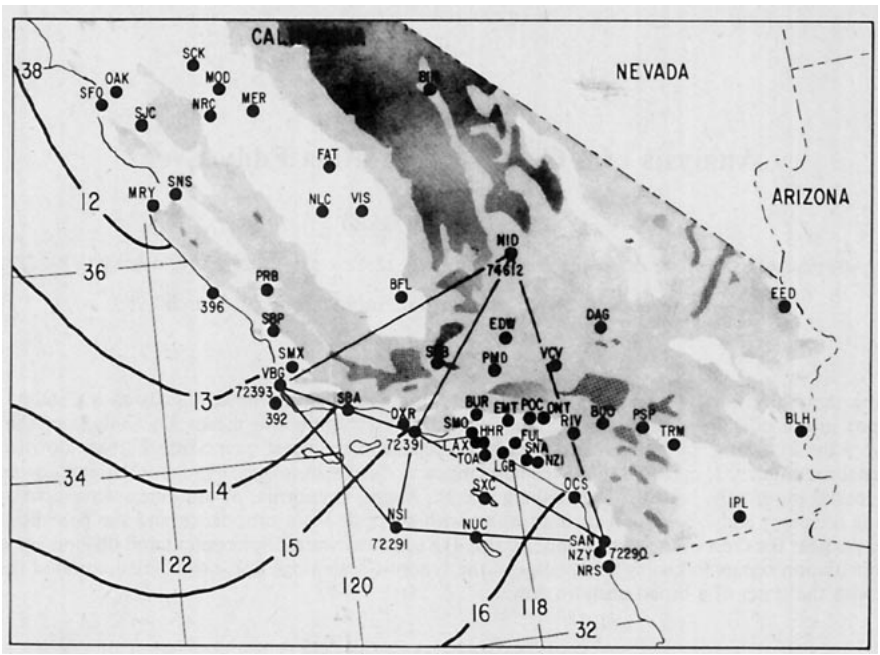

FIG. 1. Southern California location map. Standard United States three letter designators as indicated. Radiosonde stations also indicated by standard WMO designators. Dashed lines bound triangles for which kinematic computations are discussed in the text. A late May climatological sea surface temperature analysis (°C) is shown. Elevations between 300 and 1500 m (greater than 1500 m) are lightly (moderately) shaded.

gratory short wave trough approaching Oregon and northern California behind a similar trough in Arizona. Substantial ridging occurs in the next 24 h (not shown) as heights rise by 30 to 90 m along the coast. Temperature rises by 5–6°C in southern California despite continued cold advection, suggestive of large scale subsidence. Little additional change is seen in the next 24 h (0000 GMT 27 May) except for a veering and weakening of the coastal winds and the eastward spread of the ridging to the intermountain region.

By 0000 GMT 28 May (not shown) the 700 mb ridge line has advanced inland to be located from Idaho to the Gulf of California. Light southerly to southeasterly flow develops along the coast south of Vandenberg. The satellite composites (Fig. 2) suggest that the incipient cloud development occurs from 6 h before to 18 h after this time. Finally, cloud coverage is nearly complete by 0000 GMT 29 May when the 700 mb map reveals a light south to southeasterly flow across southern California with the ridge having advanced to just west of the continental divide.

The 200 mb map series depicts the northward retreat of the westerlies in advance of the ridge line which crosses the coast shortly after 0000 GMT 27 May. Comparison with the satellite information (Fig. 2) shows that the eddy circulation (as measured by the cloud distribution) commences beneath southwesterly flow in the upper troposphere. Synoptic

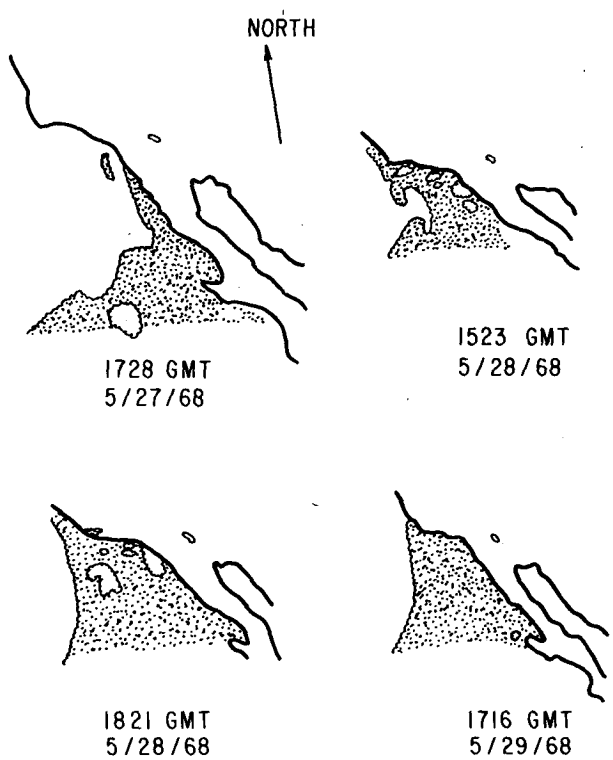

FIG. 2. Outline of stratus clouds (stippled) in the off-shore waters of California and Mexico at the indicated times. Redrawn from Rosenthal (1968).

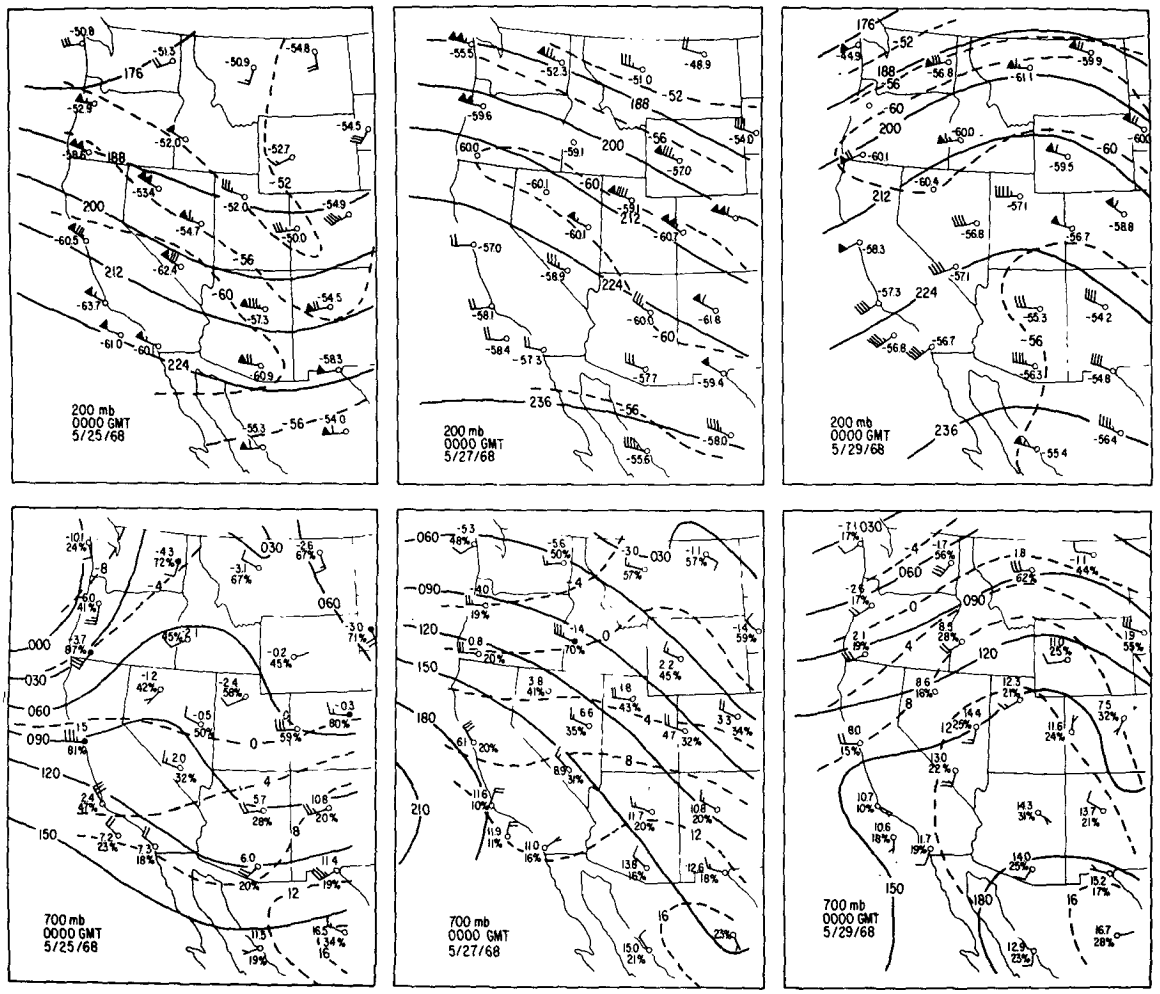

FIG. 3. Maps, 200 mb (top), and 700 mb (bottom) at 0000 GMT 25 (left), 27 (middle) and 29 May 1968 (right). Heights (solid lines) in meters at 30 and 120 m intervals on the 700 and 200 mb surfaces respectively. Isotherms (dashed lines) every 4°C. Plotted winds in m s^{-1} with one full pennant, full barb and angled barb denoting 25 m s^{-1}, 5 m s^{-1} and 2.5 m s^{-1} respectively.

scale subsidence, as forced by the implied upward increase in anticyclonic vorticity advection, is characteristic of much of the middle troposphere in the pre-circulation environment of the southwestern United States.

The synoptic scale surface map (not shown) is characterized by relatively low pressure over the intermountain region, southern Rockies and off of the Oregon coast at 0000 GMT 25 May. An anticyclone centered at 30°N, 130°W produces a northwesterly geostrophic flow from Vandenberg southward. In the ensuing 24 h pressure rises by 10–12 mb over Oregon and Washington with little change elsewhere, resulting in a strengthened northerly geostrophic gradient along the coast. By 0000 GMT 27 May the ridging spreads inland to the northern Rockies, while pressure lowers to the south with a thermal low now evident in the Imperial Valley of southern California. General pressure falls of 4–6 mb take place in the next 24 h with the thermal trough now better defined and extending northward through the San Joaquin valley. Continued pressure falls result in a relatively featureless synoptic scale weather map by 0000 GMT 29 May although, as will be shown later, the mesoscale eddy circulation is well developed.

A series of maps depicting winds, pressure and Montgomery streamfunction on the θ = 300 and 310 K isentropic surfaces are shown in Fig. 4 for selected time periods beginning 0000 GMT 27 May 1968. The purpose of these analyses is to reveal important subsynoptic features associated with eddy formation in the southern California region. Orographic penetration of the θ = 300 K surface (and sometimes θ = 310 K) by the coastal mountain ranges is not shown so caution is advised in any mesoscale interpretation of Fig. 4.

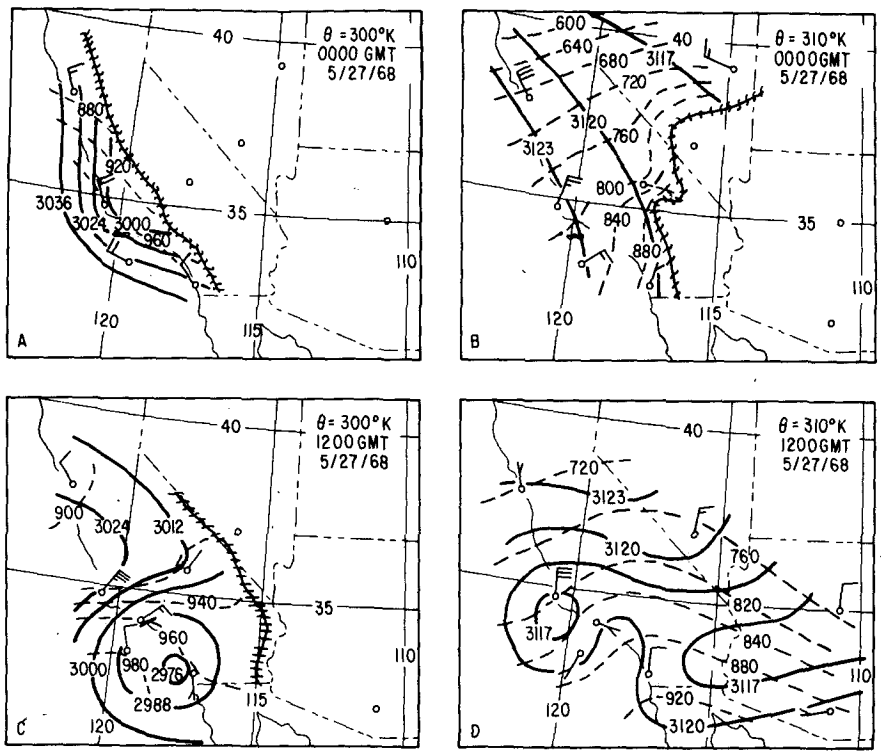

FIG. 4a. Isentropic analyses on the θ = 300 K (left), and θ = 310 K (right) surfaces for 0000 and 1200 GMT 27 May 1968. Montgomery streamfunction (solid lines, 10 $m^2 s^{-2}$) and pressure (dashed lines, mb). Plotted winds in m s^{-1} as in Fig. 3.

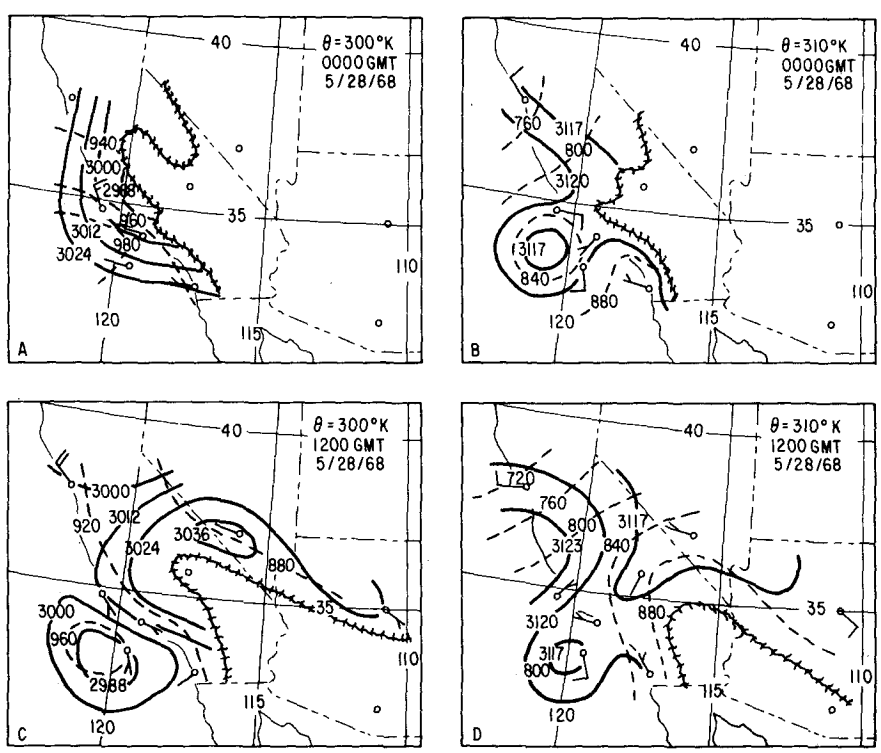

FIG. 4b. As in Fig. 4a except for 0000 GMT and 1200 GMT 28 May 1968.

At 0000 GMT 25 May 1968 the θ = 300 K and 310 K maps (not shown) reveal subsidence in the 800–900 mb layer along the southern California coastal waters and in the 725–624 mb layer across northern California in the wake of a trough passage, respectively. By 0000 GMT 27 May subsidence continues on the θ = 310 K surface along the coastal strip from San Francisco (SFO) to Los Angeles (LAX). The wind field suggests diffluence along the immediate California coast with a large component of the flow towards higher values of Montgomery streamfunction at Vandenberg (72393) and San Nicolas Island (72291). At the lower θ = 300 K level, there is the suggestion of the development of cyclonic flow just above the surface in the southern California offshore waters.

A dramatic change occurs in the following 12 h with a pronounced cyclonic circulation evident between San Nicolas Island and San Diego (72290) on the θ = 300 K surface. Subsidence continues from Vandenberg to Pt. Mugu (72391) and offshore to San Nicolas Island. The cyclonic circulation is now present on the θ = 310 K surface in the 850–800 mb layer with the center of the circulation west of a Pt. Mugu–San Nicolas Island line. The winds at Vandenberg remain strong and highly ageostrophic with subsidence still indicated west of the cyclonic circulation center.

By 0000 GMT 28 May the closed nature of the cyclonic circulation disappears on the θ = 300 K surface, probably a reflection of the afternoon sea breeze regime. Little change is evident on the θ = 310 K surface except for the relaxation of the strong Vandenberg wind. Finally, by 1200 GMT 28 May southerly wind components are seen from San Diego to Vandenberg on the θ = 300 K surface. The sense of the cyclonic circulation is now farther offshore than it was 24 h earlier. The expansion of stratus and fog northwestward along the coast (recall Fig. 2) occurs at this time. Little further change takes place on the θ = 310 K surface. Note, however, the continuation of anticyclonic curvature in the area bounded by San Nicolas Island, Pt. Mugu and San Diego.

3. Local analysis

Detailed 12 h southern and central California surface sectionals are shown in Fig. 5 for the period beginning 0000 GMT 25 May. The pressure analyses are constructed on the basis of the reported altimeter settings. Initially, California is under a northwesterly flow regime that is interrupted by an afternoon sea breeze at favorable locations. As is often the case, the Los Angeles basin is frequented by low visibilities due to pollution. Altocumulus standing lenticularis clouds over the Sierras are manifestations of the strong flow

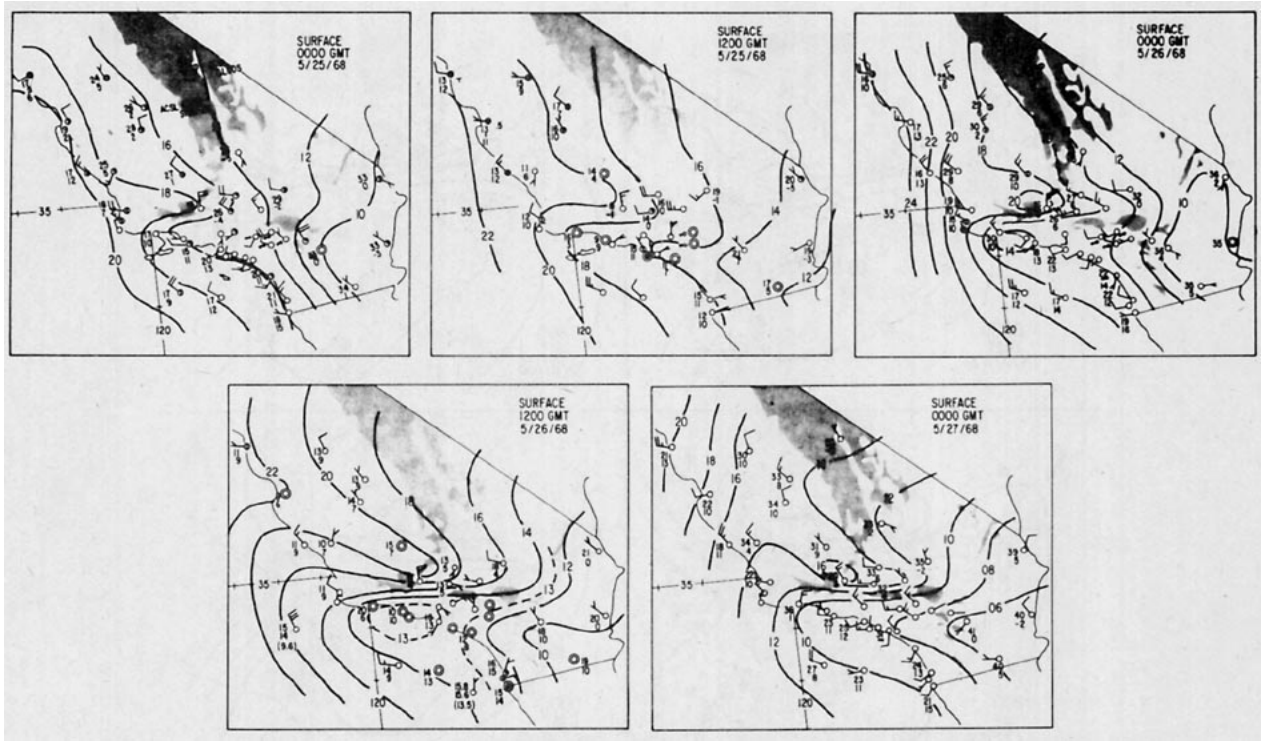

FIG. 5. Southern California surface sectionals at 12 h intervals for the period beginning 0000 GMT 25 May 1968. Isobars (solid lines) based on altimeter setting every 2 mb. Temperatures and dew points in °C. Station model according to international convention. Plotted winds as in Fig. 3. Elevations in excess of 1500 m are stippled.

aloft indicated in Fig. 3. A feature of later interest is the suggestion of a coastal trough from Los Angeles to Vandenberg to the lee of the coastal mountains. Offshore, strong northwesterlies are evident.

This general pattern continues in the next 12–24 h with increased evidence for an incipient cyclonic circulation just offshore from Santa Barbara. The northerly flow and relatively warm temperature at Santa Barbara are suggestive of downslope flow to the lee of the Santa Ynez and San Rafael mountains. Strong northerly flow at Sandberg (elevation 1357 m) in the eastern extension of these mountain ranges is a further clue to this effect.

Confirmation of the above trends is seen at 1200 GMT 26 May and 0000 GMT 27 May. A weak cyclonic circulation is well defined southeast of Santa Barbara at 1200 GMT 26 May. This circulation appears to expand southeastward 12 h later, accompanied by the development of more southerly wind components from San Diego to Los Angeles. Extensive coastal cloudiness is not yet visible in agreement with the satellite observations of Fig. 2. Overall, the general northwesterly geostrophic flow is relaxing, accompanied by extensive warming as ridging takes place aloft (Fig. 3).

Figs. 6 and 7 depict detailed coastal sectionals at 6 h intervals beginning 0600 GMT 27 May. During this period the weak cyclonic circulation expands seaward and becomes firmly established. Easterly surface wind components are evident at the offshore island locations by 0600 GMT 28 May. Comparison with Fig. 2 clearly establishes that the cyclonic circulation develops and expands in areal extent offshore *prior* to the development and organization of the stratus cloud deck. The cloud pattern associated with the eddy circulation is fully developed by 1200 GMT 29 May (not shown). In the following 48 h this cyclonic circulation slowly dissipates as a general onshore flow pattern develops in the wake of the retreating ridge aloft.

A sequence of hourly pressure readings based upon altimeter settings is shown in Fig. 8 for Sandberg, Santa Barbara, Point Mugu, and San Nicolas Island (some 3 h data at this station). Considerable diurnal, semi-diurnal and other small scale variations are superimposed upon the synoptic scale pressure trace. The general pressure minimum in the vicinity of 0000 GMT 28 May coincides with the passage of the synoptic scale ridge line aloft. It is indicative of surface pressure falls in response to subsidence warming aloft. The implied pressure difference between Sandberg (elevation 1357 m) and the coastal stations is largely artificial. The inland lower troposphere increasingly departs from the standard atmosphere as general warming develops (recall Fig. 5) whereas the reverse is true in the opposite sense at coastal stations as the

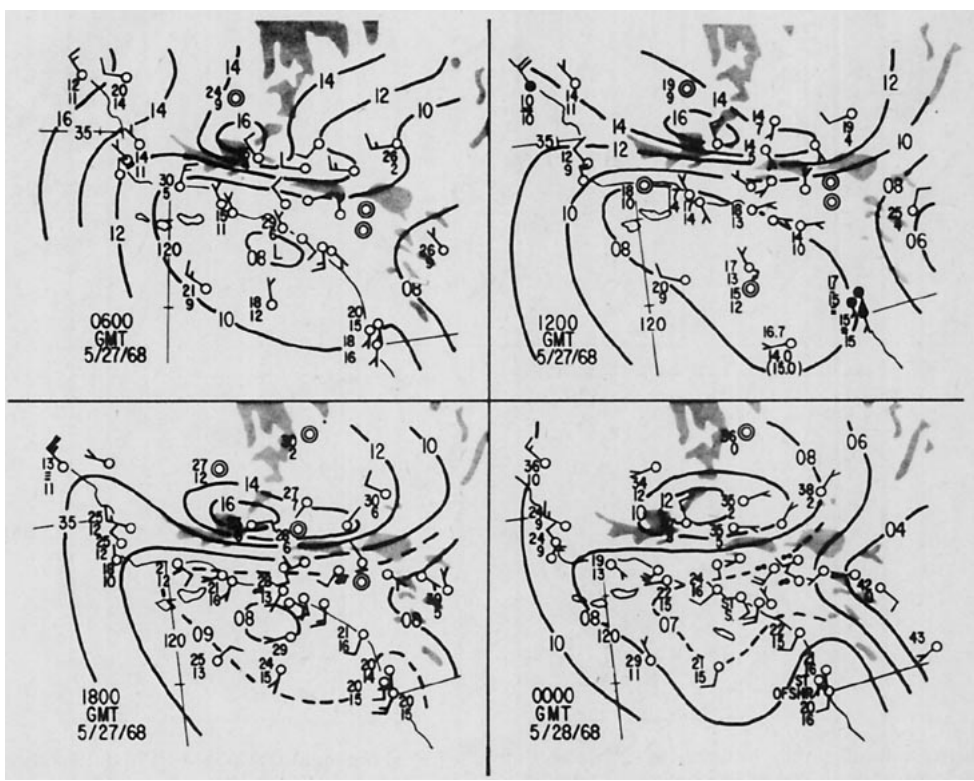

FIG. 6. As in Fig. 4 except for 6 h periods beginning 0600 GMT 27 May 1968.

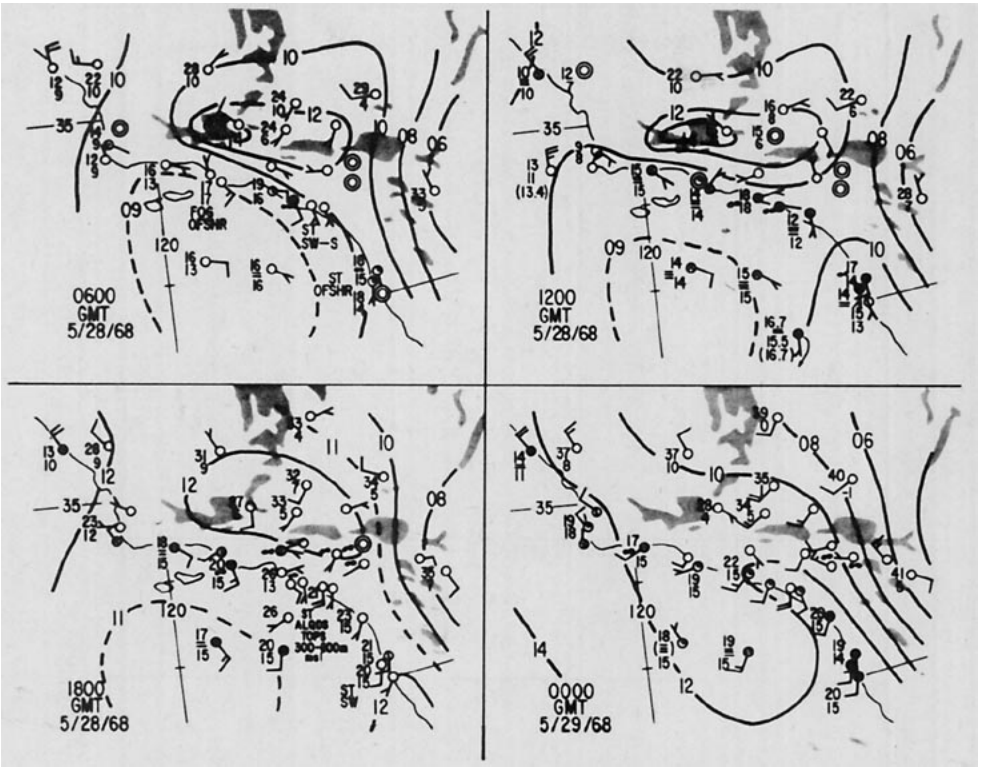

FIG. 7. As in Fig. 4 except for 6 h periods beginning 0600 GMT 28 May 1968.

marine layer deepens and the inversion strengthens. The combination of these two effects account for 3–6 mb of the implied pressure difference. This difference begins to decrease again on 29 May after the eddy circulation is fully developed and a general onshore flow pattern arises which somewhat reduces the magnitude of coastal versus inland thermal gradient.

Marine air occupies San Nicolas Island (elevation 171 m) prior to 1200 GMT 26 May and after 0000 GMT 28 May (see Fig. 9). During the afternoons of 26 and 27 May the surface station lies in the "warm" air just above the shallow marine inversion. In either case the altimeter setting is probably a very good representation of the mean sea level pressure. According to Fig. 8, San Nicolas Island tends to average slightly higher in pressure than either Santa Barbara (SBA) or Pt. Mugu from 1800 GMT 25 May through 0300 GMT 27 May, except around 0600 GMT 26 May when marine air exists at Santa Barbara (see Fig. 9). This period coincides with incipient eddy formation. The reverse is often true after 0000 GMT 28 May during which time the eddy circulation expands seaward (recall Fig. 5) as easterly wind components are seen at the offshore island locations. This represents additional evidence that the initial pressure minimum forms very close to the coast and not well offshore.

Fig. 9 depicts the 3 h wind, temperature, and cloud observations (intermediate data plotted where appropriate) for Santa Barbara, San Nicolas Island and San Diego. Santa Barbara is clearly influenced by downslope winds during the afternoon hours of 25 and 26 May. The reported winds are extremely variable on

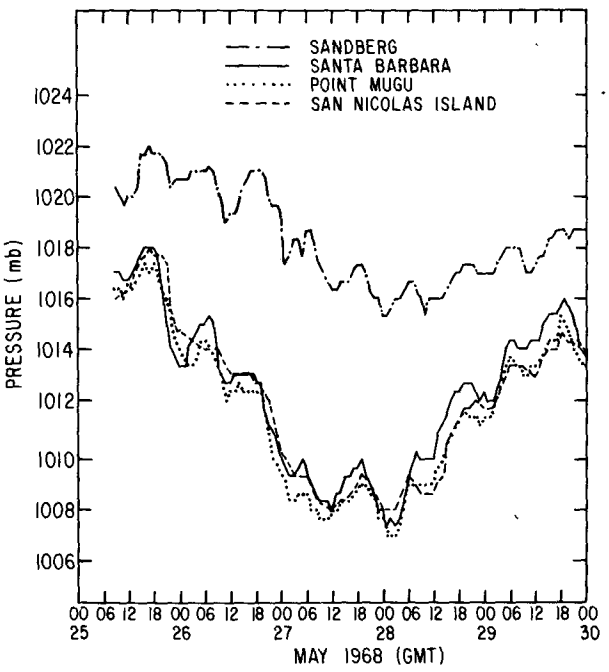

FIG. 8. Pressure (mb) based on altimeter setting versus time (GMT) for four California stations.

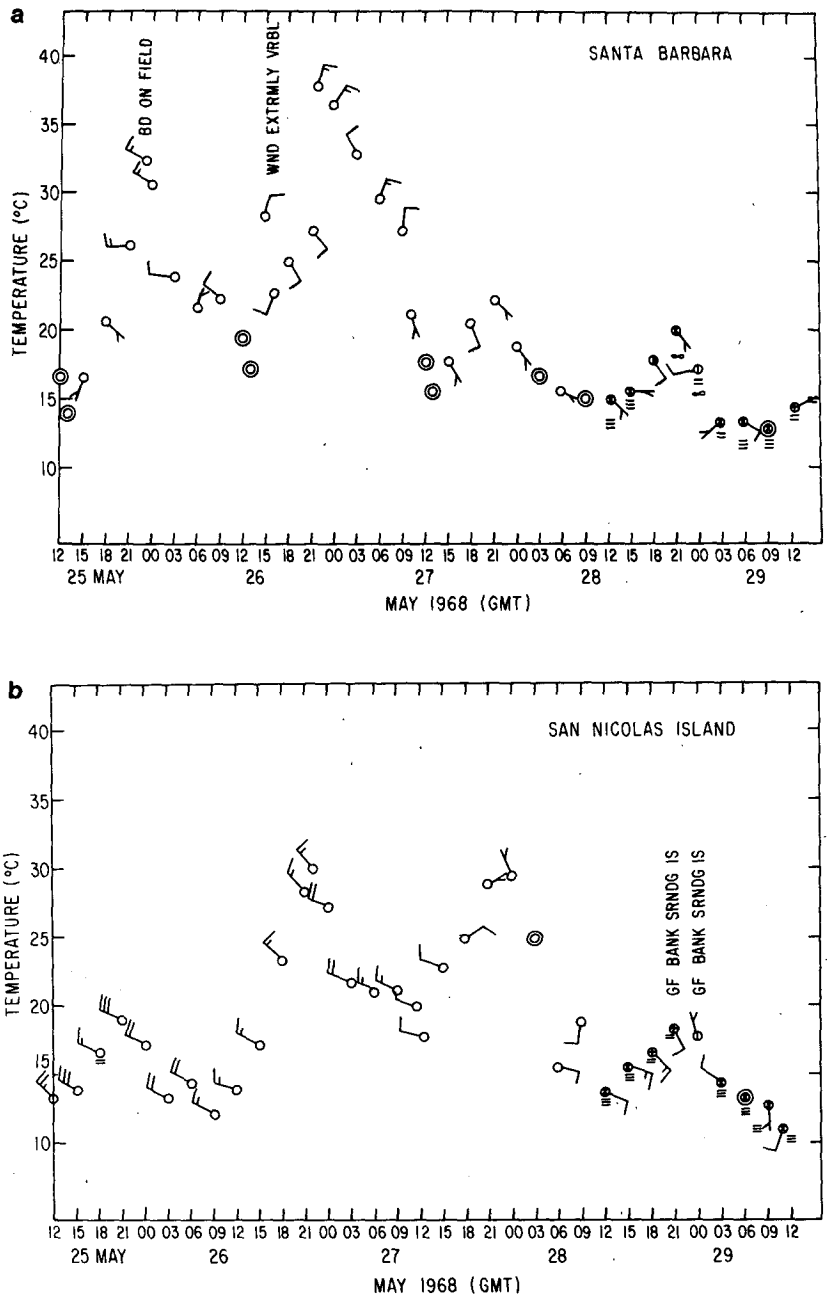

FIG. 9. As in Fig. 8, except for temperature (°C), wind (m s^{-1}), sky condition and present weather at (a) Santa Barbara, (b) San Nicolas Island and (c) San Diego.

the latter day with abrupt early morning temperature rise and a north-northwest wind followed by an abrupt midmorning temperature fall with an onshore flow. The downslope flow returns spectacularly by midday with the temperature peaking at 39°C. Sustained southeasterly flow reaches Santa Barbara after 1200 GMT 27 May with low cloud and fog associated with the evolving eddy circulation rolling in 24 h later. During this period the reported ceilings increase from below 100 m to almost 200 m.

At San Nicolas Island, northwesterly flow prevails through 0900 GMT 27 May with a general warming trend. Subsequently the westerly winds weaken, veer to northerly and become calm by 0300 GMT 28 May. The first easterly components appear at 0600 GMT 28 May accompanied by a spectacular temperature plunge. Fog and low cloud dominate the picture during the remainder of the period except around 0000 GMT 29 May when the observer reports undercast conditions.

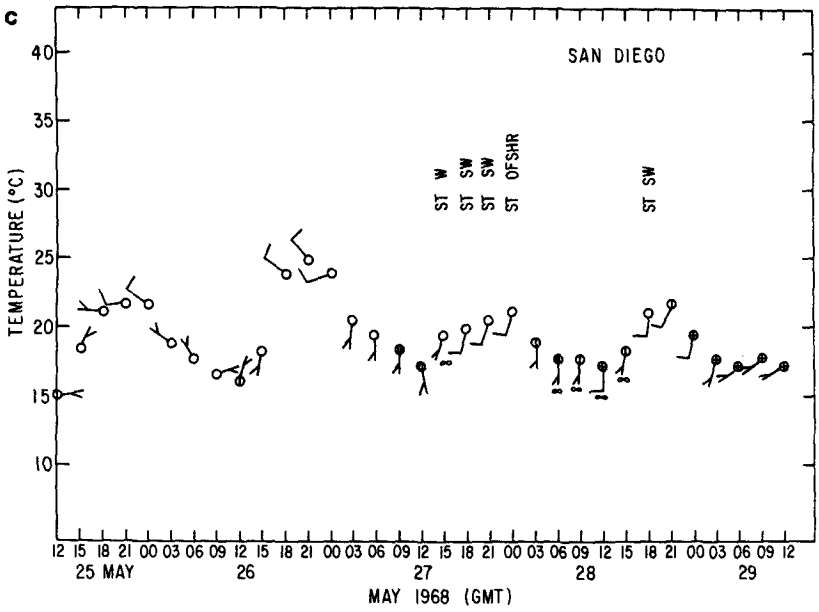

FIG. 9. (*Continued*)

At San Diego, westerly flow is interrupted by 0300 GMT 27 May with continued southerly flow thereafter, gradually veering to more southwesterly by 29 May. The nocturnal offshore wind regime is conspicuously absent. The southerly flow is most pronounced during the midday hours on 28 May as the eddy circulation becomes well developed. Reported ceilings are in the range of 400–500 m on 29 May (they had been in the 100–150 m range 24–48 h earlier), indicative of the deepening of the marine layer.

4. Vertical structure

A vertical time section of wind and potential temperature for Vandenberg based upon 6 h sounding data is shown in Fig. 10. Strong winds initially in the mid and upper troposphere weaken and back (veer) to southwesterly above (below) 400 mb as the ridge line aloft passes on 27 May. Warming and drying in the lower troposphere is most pronounced in the 12 h ending 0000 GMT 26 May. A prominent feature is the development of relatively strong northerly and northeasterly winds (the highest speeds in the sounding) in the 900–700 mb layer in the 36 h period beginning 0000 GMT 26 May. A downward propagation of the wind maximum accompanied by veering is suggested for the 900–700 mb layer with the greatest winds near mountain top level on 27 May. Further warming also takes place. Inspection of the 850 mb maps (not shown) discloses that the strong lower tropospheric winds are supergeostrophic and blow towards higher heights. Additional sounding data taken from nearby sounding stations on Vandenberg Air Force Base [not shown, e.g., Pt. Arguello—(72392)] show similar wind profile credibility to Fig. 10. This curious feature is perhaps a "corner" effect in response to flow around the west end of the Santa Ynez mountains. It appears well correlated with the Ba-

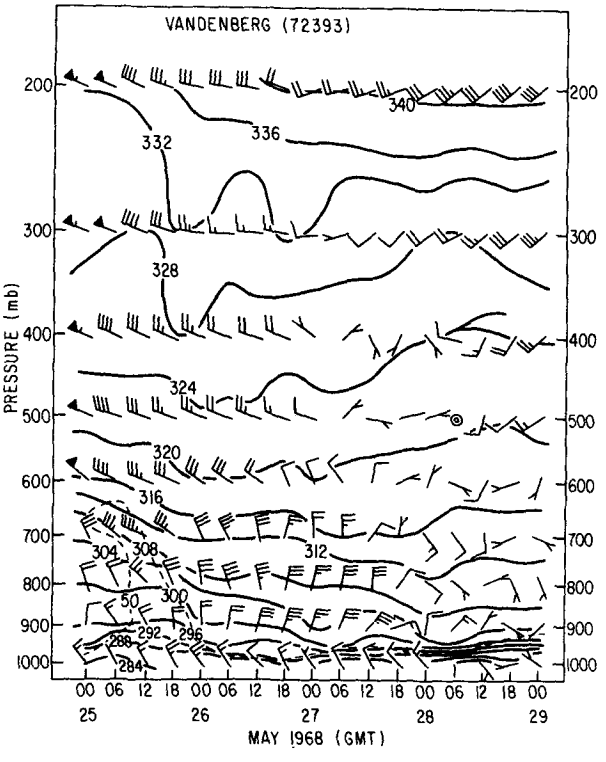

FIG. 10. Time cross section of potential temperature (K) and wind (m s^{-1}) at Vandenberg, California (72393). Potential temperature contoured every 4 K. Winds plotted as in Fig. 3. Dashed line denotes areas with a relative humidity greater than 50%. Time (GMT) along the abscissa.

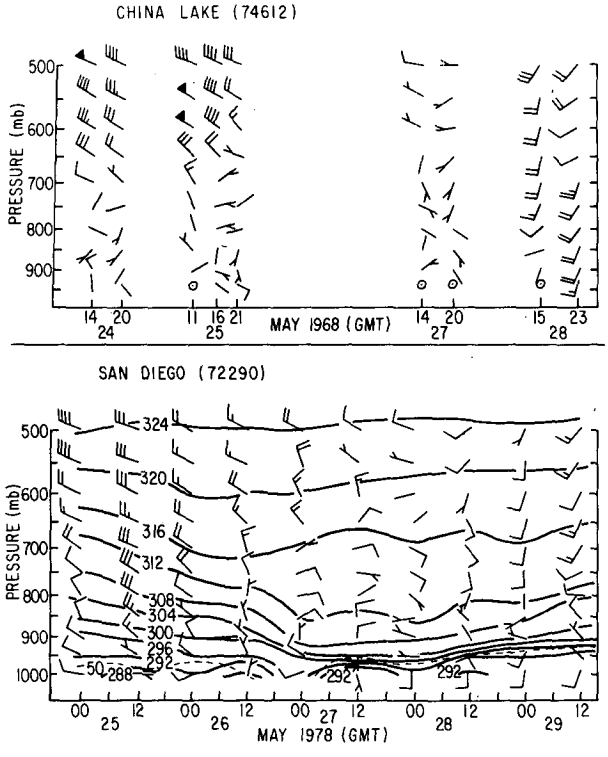

FIG. 11. As in Fig. 10, except for China Lake (74612) at the top, and San Diego (72290) at the bottom. Only winds are plotted for the irregular China Lake observations.

kersfield (BFL)–Los Angeles pressure difference with strong lower tropospheric winds at Vandenberg occurring with higher pressure at Bakersfield. Finally, note the development and deepening of the marine layer with time, particularly after 0000 GMT 28 May.

An irregular series of wind observations for China Lake (north of the coastal mountains) and winds and potential temperature for San Diego is shown in Fig. 11. The weakening of the winds accompanied by warming at China Lake between 1100–2100 GMT 25 May in the 700–550 mb layer is in agreement with the Vandenberg observations. While a data gap precludes a definitive statement, it seems reasonable to conclude that strong low level winds at China Lake are absent. This represents additional evidence for a significant topographical influence on the Vandenberg winds. At San Nicolas Island (Fig. 12) the average 900–700 mb layer wind veers from northwest at 1200 GMT 26 May to northeast at 0000 GMT 27 May. Average wind speeds are between 7–8 m s^{-1} at both times. Meanwhile San Diego experiences a similar warming on both 26 and 27 May. The marine layer is firmly established by 1200 GMT 27 May, deepening gradually thereafter.

A number of other features are worthy of comment. At 1200 GMT 27 May low level (950–800 mb) winds have easterly components both at Vandenberg and Pt. Mugu, whereas at San Nicolas Island (aside from 950 mb) light southeasterly winds have developed. Coupled with the observed surface winds this is suggestive of a weak cyclonic circulation that tilts westward with height, an idea supported by the isentropic analyses in Fig. 4. The evolving wind field at San Nicolas Island thereafter is consistent with the idea of an expanding cyclonic circulation to the south. Another curious feature is the occurrence of light northwesterly winds at San Diego, San Nicolas Island and Pt. Mugu between 900 and 800 mb by 0000 GMT 29 May and especially 12 h later. Meanwhile, winds in the same layer at Vandenberg remain more southerly through 0600 GMT 29 May (not shown) and light northeasterly by 1200 GMT 29 May (also not shown), suggestive of a weak anticyclonic circulation just above the top of the marine layer. Evidence for this anticyclonic is seen on the $\theta = 310$ K surface (Figure 4b) as early as 0000 GMT 28 May.

Selected vertical sounding profiles for Vandenberg and San Nicolas Island are shown in Figs. 13 and 14, respectively. Particularly impressive is the appreciable warming below 500 mb at Vandenberg in the 24 h ending 0000 GMT 26 May. Earlier it was remarked in connection with Fig. 3 that 700 mb warming took place despite implied cold advection and that subsidence was the most likely source of the warming. Confirmation is seen in Fig. 15 which gives the result of an adiabatic calculation of vertical motion at 700 mb at 34.5°N, 120.0°W (on the coast between Santa Barbara and Vandenberg) using a one degree lati-

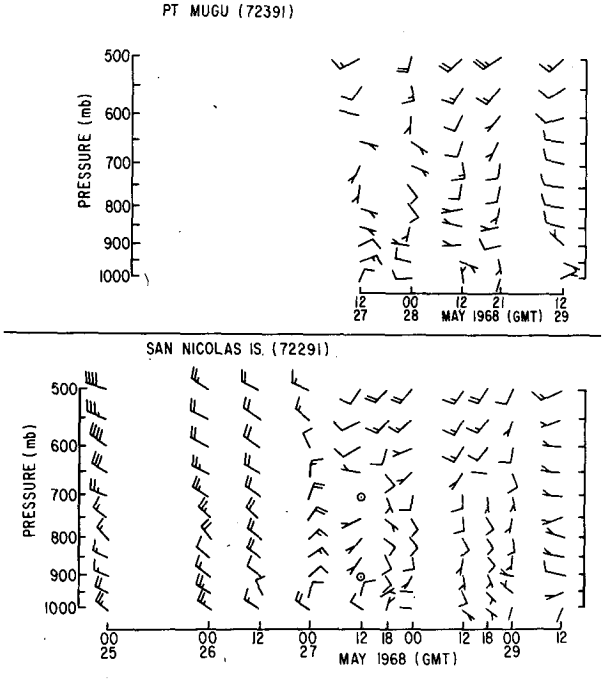

FIG. 12. As in Fig. 10, except for Point Mugu (72391) at the top, and San Nicolas Island (72291) at the bottom. Winds only.

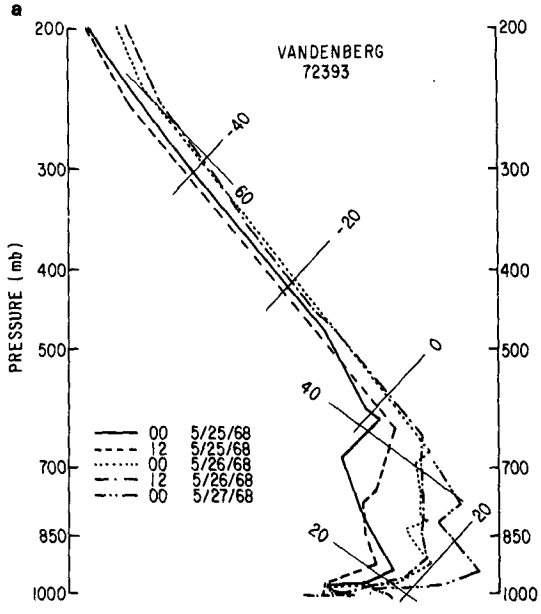

FIG. 13a. Vandenberg (72393) temperature soundings at 12 h intervals, skew T-log p format, beginning 0000 GMT 25 May 1968. Isotherms (°C) and isentropes (°C) slope upward to the right and left, respectively.

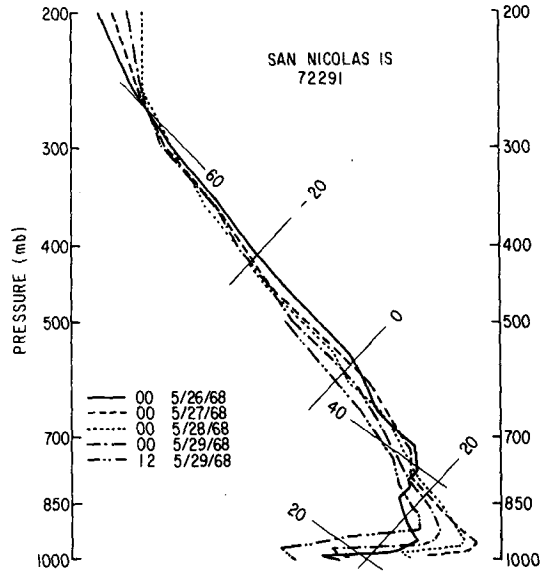

FIG. 14. As in Fig. 13a, except for San Nicolas Island (72291) and dates as shown.

tude–longitude centered finite difference computation. The local temperature tendency was taken as a 6 h difference using the reported Vandenberg 700 mb temperatures. Subsidence amounting to 4×10^{-3} mb s^{-1} ($\approx$4 cm s^{-1}) is seen through 0000 GMT 27 May yielding to ascent 24–36 h later as the ridge line advances eastward. Descent of this magnitude will produce a 12 h warming of the 8–10°C in the 600–800 mb layer according to the sounding in Fig. 13. The horizontal cold advection implies a cooling of ~6°C (12 h)$^{-1}$ yielding a net warming of 2–4°C (12 h)$^{-1}$, in reasonable agreement with observation.

The warming is accompanied by the development of a pronounced stable layer between 900 and 700 mb which persists through 1200 GMT 27 May. The presence of the stable layer in conjunction with relatively strong winds perpendicular to the crests of the

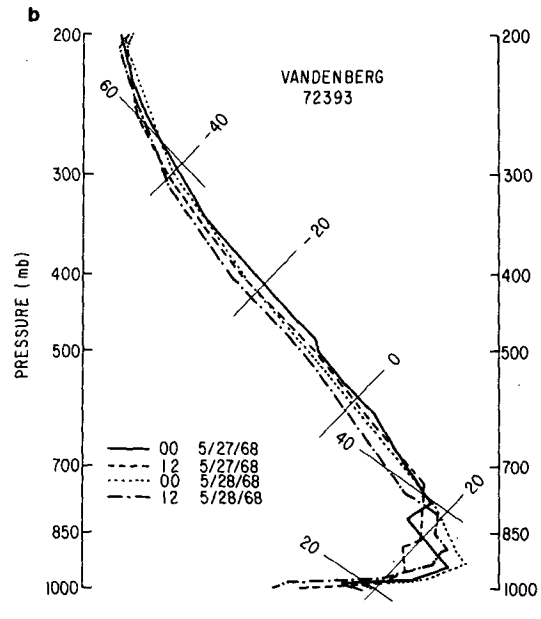

FIG. 13b. As in Fig. 13a, except for dates as shown.

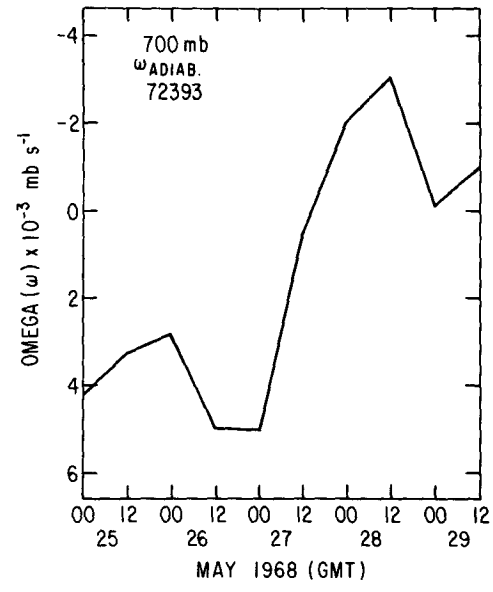

FIG. 15. Time series of 700 mb adiabatic vertical motion valid at 34.5°N, 120°W on the California coast between Santa Barbara and Vandenberg. Time (GMT) along abscissa. Units: 10^{-3} mb s^{-1}.

coastal mountains raises the possibility of a mountain wave influence on the offshore eddy circulation. A similar stable layer is weakly evident at San Nicolas Island prior to 0000 GMT 28 May. Finally, the development and growth of the marine boundary layer is observed at San Nicolas Island and more weakly at Vandenberg, as the eddy circulation evolves.

5. Kinematic analyses

Kinematic computations of vertical motion and relative vorticity were made for selected triangles defined by available radiosonde stations, using the computational method described by Bosart and Sanders (1981). Input winds consisted of surface values and values at every 50 mb thereafter to 100 mb. This approximately accounts for the effect of orography. The vertically integrated divergence was corrected to zero (constant correction) with an assumed upper boundary condition of the vertical motion vanishing at 100 mb.

The first available computations are for 0000 GMT 26 May and are shown in Fig. 16. Both the Vandenberg–San Nicolas Island–China Lake and San Nicolas Island–San Diego–China Lake triangles exhibit cyclonic (anticyclonic) vorticity in the lower (upper) troposphere. The cyclonic vorticity reflects the relatively strong low level winds at Vandenberg and San Nicolas Island, whereas the anticyclonic vorticity is an indication of ridge conditions aloft on the anticyclonic shear side of the wind maximum. Weak ascent is suggested in both triangles below 800 mb with weak descent above in the eastern triangle.

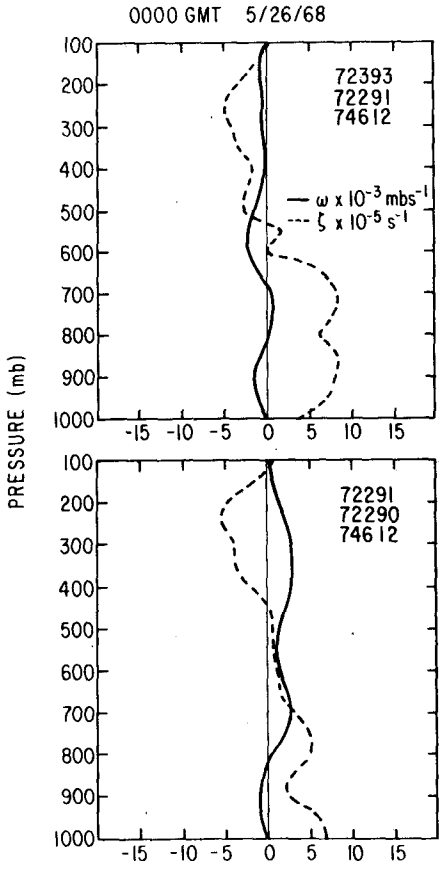

FIG. 16. Kinematic computation of vertical motion, and relative vorticity at 0000 GMT 26 May 1968 for radiosonde triangles bounded by Vandenberg (72393), San Nicholas Island (72291) and China Lake (74612) at the top; San Nicholas Island (72291), San Diego (72290) and China Lake (74612) at the bottom.

An interesting picture emerges 36 h later at 1200 GMT 27 May, corresponding to a well developed cyclonic eddy circulation in the absence of significant cloud (recall Fig. 6). The results are shown in Fig. 17 for four triangles of varying shape and size, but caution is advised in the interpretation. Pronounced ascent through 400 mb is implied in both smaller over-water triangles. The result must be viewed with considerable suspicion, however, because the computations are sensitive to the relatively strong low level northeasterly winds at Pt. Mugu and especially Vandenberg (recall Figs. 10–12). The cyclonic vorticity profile in the Vandenberg–Pt. Mugu–San Nicolas Island triangle below 500 mb is undoubtedly influenced by the Vandenberg winds. Broad subsidence is seen inland in the Pt. Mugu–San Diego–China Lake triangle. Weak midlevel ascent is computed to the west (Vandenberg–Pt. Mugu–China Lake). In all cases, however, the air is far too dry to produce visible cloud despite any implied ascent.

Similar vertical motion and relative vorticity profiles were prepared (not shown) for the Vandenberg–San Nicolas Island–Pt. Mugu and Pt. Mugu–San Nicolas Island–San Diego triangles for 1200 GMT 28 May, 0000 and 1200 GMT 29 May. The eddy is at maximum strength early in this period, gradually decaying thereafter. Both 1200 GMT profiles indicate deep, but weak ascent, particularly on 28 May. Descent is indicated at 0000 GMT 29 May (above 900 mb in the Vandenberg–Pt. Mugu–San Nicolas Island triangle) throughout much of the troposphere. Perhaps the alteration in the sign of the vertical motion is a manifestation of a sea breeze modulation of the eddy circulation. The limited satellite information (Fig. 2) does not suggest a cloud cover amount reduction and is incapable of resolving any cloud thinning. However, the San Nicolas Island time section (Fig. 9b) implies a reduction in cloud cover and a lowering of cloud tops at the top of the marine layer in the vicinity of 0000 GMT 29 May.

6. Remarks and concluding discussion

We have examined in detail the life cycle of a cyclonic eddy (known locally as a Catalina eddy) in the marine layer in the offshore waters of southern California for 26–29 May 1968. Interest in the case was stimulated by Rosenthal's (1968) publication of satellite pictures of the event.

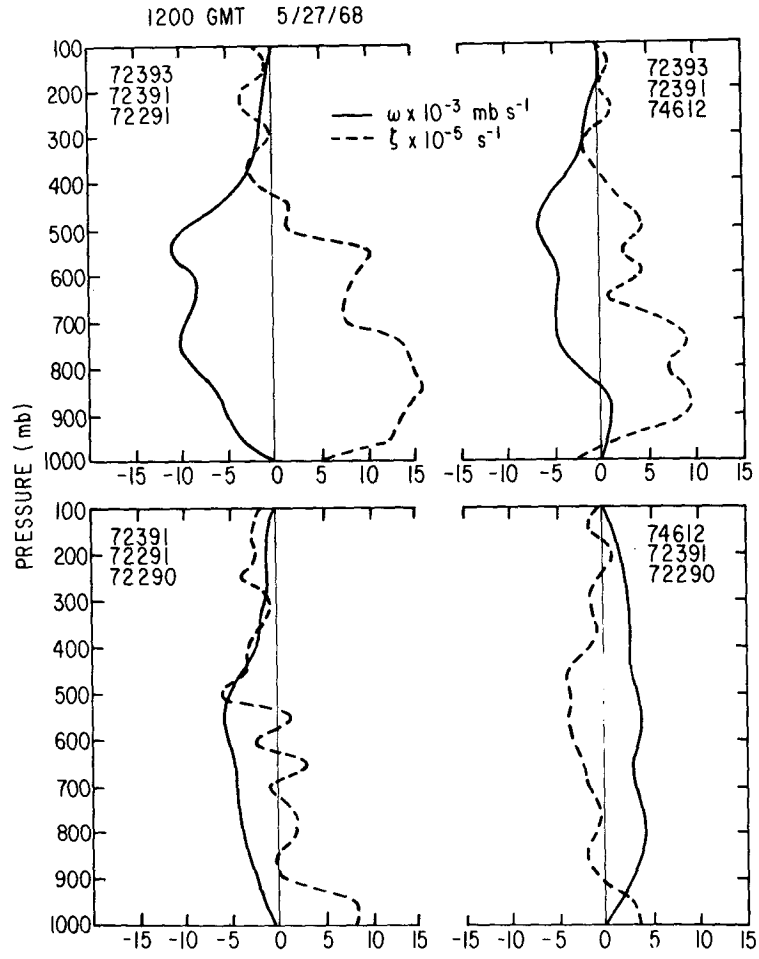

FIG. 17. As in Fig. 15, except for 1200 GMT 27 May 1968. Upper left: Vandenberg, Point Mugu, San Nicolas Island; Upper right: Vandenberg, Point Mugu, China Lake; Lower left: Point Mugu, San Nicolas Island, San Diego; Lower right: China Lake, Point Mugu, San Diego.

A principal finding is that the initial pressure minimum forms on the coast in the vicinity of Santa Barbara. Careful analysis shows that surface pressures (based on altimeter settings) are slightly higher at the offshore island locations. At this time the synoptic scale surface map reveals a broad northwesterly flow which satisfies a criterion specified by Eichelberger (1971) for the occurrence of a Catalina eddy. The initial pressure minimum forms *prior* to the passage of the synoptic scale ridge line aloft. The southern California region at this time is favored by synoptic scale subsidence. Kinematic and adiabatic vertical motion calculations verify the observed synoptic scale warming at the surface and aloft. This is in marked contrast to the generally weak trough conditions in the mid-troposphere found by Eichelberger (1971) to be characteristic of eddy situations.

Inspection of the soundings at the time of the appearance of the initial pressure minimum reveals characteristics associated with classical mountain waves. At Point Mugu, San Nicolas Island and especially at Vandenberg there is ample evidence of a relatively strong low-level flow from the north-northeast (averaging 10–20 m s^{-1}) perpendicular to the coastal mountain ranges. Surface reports from Santa Barbara reveal extremely variable winds alternating between onshore and offshore. Gusty offshore winds at Santa Barbara send the temperature soaring to just under 40°C, clear evidence of a downslope transit for the air. Additionally, sounding data downwind of the coastal mountains at San Nicolas Island and Pt. Mugu reveals the presence of a weak stable layer in the vicinity of the mountain crests. The stable layer is also present at Vandenberg to the west of the Santa Ynez mountains but downwind of lower mountains to the north. This stable layer, likely produced by subsidence and low-level divergence in the presence of an elevated lower boundary upstream, is characteristic of mountain wave episodes. Colson (1954), Brinkman (1974), Klemp and Lilly (1975, 1978), and

Lilly (1978) have commented on the observational and theoretical importance of the mountain crest stable layer in connection with Colorado windstorms. Unlike Colorado windstorms however, a large amplitude wave is absent over and downwind of the mountains. The role of the vertical propagation of gravity wave energy generated by the mountains, if any, is far from obvious in the California case.

Sommers (1978) has shown the existence of similar stable layers in association with episodes of downslope Santa Ana winds in California. The Santa Ana wind typically develops in the wake of a moderately vigorous trough passage aloft when sea level pressures rise in the Great Basin area to levels substantially higher than along the southern California coast. Synoptic scale subsidence is present over a broad area during a Santa Ana wind episode. In this context the formation of a center of low pressure on the coast between Point Mugu and Vandenberg is remarkably similar to what might be expected for a very localized Santa Ana wind condition. Indeed, the 200 mb pattern shown in Fig. 3 is commonly associated with at least a weak Santa Ana regime. Upstream documentation of the stable layer is difficult. Soundings were not available from Edwards Air Force Base during the crucial time from 25 to 27 May. However, China Lake observations at 1832 and 2215 GMT 25 May revealed the presence of a stable layer (average temperature decrease of 7.5°C) in the 730–570 mb layer, a vertical distance of ~2000 m. Winds were northwesterly between 10–15 m s^{-1} in the upper half of this stable layer.

Once formed, the pressure minimum expands seaward and southeastward resulting in a well defined cyclonic circulation in the marine layer. The expansion of the cyclonic circulation occurs in conjunction with the passage of the ridge line aloft and the cessation of synoptic scale subsidence. A colleague who grew up in Southern California, J. M. Brown (personal communication, 1983) has suggested that two interesting springtime processes may be playing significant roles in eddy formation. First, air flow over the coastal mountain ranges, even though it may not be manifest as a large-amplitude wave, can emerge more homogenous in the vertical to the lee of the mountains than it was as it approached the windward slopes. The effect of this, in conjunction with synoptic scale subsidence, is to cause the low level air to the lee of the coastal mountains to be considerably warmer than air to windward. At some level well above the mountain crests there is little or no overall change in the temperature lapse rate. This "plume" of low-level air is then much warmer than air at the same elevation that has not experienced a cross mountain trajectory (i.e., air flowing southward perhaps 100–200 km to the west of Vandenberg and San Nicolas Island). This implies lower pressure over and south of the coastline, especially to the west of Los Angeles, and the development of cyclonic shear vorticity offshore. The effect in turn may be enhanced by intense solar heating over the land at this time of the year, but its importance in this case is not obvious.

Second, the observed downslope flow at Santa Barbara suggests a mountain wave influence, perhaps localizing the warming to some extent and creating conditions favorable for slightly lower sea level pressure along the coast from Santa Barbara to Pt. Mugu than elsewhere. One possible effect of the localized warming might be to draw the offshore region of cyclonic shear vorticity closer to the coast, together with the creation of cyclonic curvature vorticity. The latter argument is not without problems. "Homogenization" of the air downwind of the coastal mountains could also lead to stronger northerlies there. This would tend to diminish the cyclonic shear vorticity farther offshore. There are obviously some geostrophic adjustment problems that are not fully appreciated at this time. It seems reasonable to say, however, that the existence of downslope flow in the vicinity of Santa Barbara is not crucial to eddy development. Rather, it is a measure of the strength and slightly anomalous character of the flow, given the time of the year.

Kinematic analysis reveals the presence of cyclonic relative vorticity from the surface to 900 mb in the mature to decaying stages of the life cycle of the eddy. During this stage weak synoptic scale ascent is present following the passage of the ridge line. A general deepening of the marine layer is observed, particularly at San Diego. Dissipation of the eddy circulation takes place with the development of a general onshore flow as the ridge line aloft retreats further eastward.

Our analysis has necessarily been restricted to a single case—so generalization should be avoided. It is obvious, however, that many of the rules of thumb described by Rosenthal (1972) for forecasting Catalina eddy development remain valid. However, the common rule of thumb that an eddy circulation begins with the first appearance of sustained southerlies at San Diego in the face of a northwesterly synoptic scale geostrophic gradient requires some modification.

Accordingly to Fig. 8c sustained southerlies begin at San Diego by 0300 GMT 27 May. Fig. 5 shows that a cyclonic circulation first appears by 0000 GMT 26 May and is well established 12 h later, 15 h prior to the appearance of southerlies at San Diego. Note, however, from Fig. 9c that southerlies did appear briefly at San Diego on the morning of 26 May and veered from westerly to southerly 12 h later. This is a very common signal that some sort of weak Catalina eddy is trying to form and, to further reinforce the previous Santa Ana discussion, is sometimes observed to distinguish the breakdown of a Santa Ana regime and its evolution into a Catalina eddy. This case is then somewhat atypical in that probably no

more than 25% of Santa Anas evolve into Catalina eddies, usually the weak ones (John M. Brown, personal communication, 1983). The author is thus hesitant to put forth any specific forecast recommendations given the somewhat atypical nature of the event.

Finally, satellite pictures, however interesting, do not reveal the whole story. The very dry air mass does not sustain widespread cloudiness until sufficient low-level convergence and ascent acts for a long enough time period. The eddy circulation, as defined by the winds, is well in evidence 24–30 h prior to any stratus signature. This does suggest, however, that a future SEASAT instrument [Jones *et al.* (1982) and Hoffman (1982)] might be very revealing for a future quantitative research investigation.

Acknowledgments. The author gratefully acknowledges stimulating conversations on weather regimes with Dr. J. M. Brown of NOAA's Office of Weather Research and Modification in Boulder, Colorado. His thorough review of the manuscript is deeply appreciated. Helpful comments were provided by the anonymous referees. Partial support for this research was provided by NASA Contract NASA1-15948 (1980) and NSF Grant ATM802655702. The manuscript was typed by Ms. Cyndie Erdt and the figures were drafted by Ms. Marilyn Peacock.

REFERENCES

Bosart, L. F., and F. Sanders, 1981: The Johnstown flood of July 1977: A long lived convective system. *J. Atmos. Sci.*, **38,** 1616–1642.

Brinkman, W. A. R., 1974: Strong downslope winds at Boulder, Colorado. *Mon. Wea. Rev.*, **102,** 592–602.

Colson, D., 1954: Meteorological problems in forecasting mountain waves. *Bull. Amer. Meteor. Soc.*, **35,** 363–371.

Eichelberger, A. L., 1971: Forecasting the Catalina Eddy. NOAA Tech. Memo., National Weather Service Western Region—COM-71-00223, 18 pp. [Available from National Weather Service Western Region, Box 11188, Federal Building, 125 South State St., Salt Lake City, UT 84111.]

Hoffman, R. N., 1982: SASS wind ambiguity removal by direct minimization. *Mon. Wea. Rev.*, **110,** 434–445.

Jones, W. L., L. C. Schroeder, D. H. Boggs, E. M. Bracalente, R. A. Brown, G. J. Dome, W. J. Pierson and F. J. Wentz, 1982: The SEASAT-A Satellite Scatterometer: The geophysical evaluation of remotely sensed wind vectors over the ocean. *J. Geophys. Res.*, **87,** 3297–3317.

Klemp, J. B., and D. K. Lilly, 1975: The dynamics of wave-induced downslope winds. *J. Atmos. Sci.*, **32,** 320–339.

——, and ——, 1978: Numerical simulation of hydrostatic mountain waves. *J. Atmos. Sci.*, **35,** 78–107.

Lilly, D. K., 1978: A severe downslope wind storm and aircraft turbulence event induced by a mountain wave. *J. Atmos. Sci.*, **35,** 59–77.

Rosenthal, J., 1968: A Catalina eddy. *Mon. Wea. Rev.*, **96,** 742–743.

——, 1972: Point Mugu forecasters handbook. Pacific Missile Range Point Mugu, CA. [Available from Geophysics Division, Pacific Missile Test Center, Point Mugu, CA 93042.]

Sommers, W. T., 1978: LFM forecast variables related to Santa Ana wind occurrences. *Mon. Wea. Rev.*, **106,** 1307–1316.